

# SEC23B is required for pancreatic acinar cell function in adult mice

Rami Khoriaty<sup>a</sup>, Nancy Vogel<sup>b,†</sup>, Mark J. Hoenerhoff<sup>c</sup>, M. Dolores Sans<sup>b</sup>, Guojing Zhu<sup>d</sup>, Lesley Everett<sup>e,‡</sup>, Bradley Nelson<sup>b</sup>, Haritha Durairaj<sup>b</sup>, Brooke McKnight<sup>f,§</sup>, Bin Zhang<sup>g</sup>, Stephen A. Ernst<sup>h</sup>, David Ginsburg<sup>a,d,i,j,\*</sup>, and John A. Williams<sup>a,b,\*</sup>

<sup>a</sup>Department of Internal Medicine, <sup>b</sup>Department of Molecular and Integrative Physiology, <sup>c</sup>In Vivo Animal Core, Unit for Laboratory Animal Medicine, <sup>d</sup>Life Sciences Institute, <sup>e</sup>University of Michigan Medical School, <sup>f</sup>College of Literature Science and the Arts, <sup>h</sup>Department of Cell and Developmental Biology, <sup>i</sup>Departments of Human Genetics and Pediatrics and Communicable Diseases, and <sup>j</sup>Howard Hughes Medical Institute, University of Michigan, Ann Arbor, MI 48109; <sup>g</sup>Genomic Medicine Institute, Cleveland Clinic Lerner Research Institute, Cleveland, OH 44195

**ABSTRACT** Mice with germline absence of SEC23B die perinatally, exhibiting massive pancreatic degeneration. We generated mice with tamoxifen-inducible, pancreatic acinar cell-specific *Sec23b* deletion. Inactivation of *Sec23b* exclusively in the pancreatic acinar cells of adult mice results in decreased overall pancreatic weights from pancreatic cell loss (decreased pancreatic DNA, RNA, and total protein content), as well as degeneration of exocrine cells, decreased zymogen granules, and alterations in the endoplasmic reticulum (ER), ranging from vesicular ER to markedly expanded cisternae with accumulation of moderate-density content or intracisternal granules. Acinar *Sec23b* deletion results in induction of ER stress and increased apoptosis in the pancreas, potentially explaining the loss of pancreatic cells and decreased pancreatic weight. These findings demonstrate that SEC23B is required for normal function of pancreatic acinar cells in adult mice.

## Monitoring Editor

Thomas F. J. Martin  
University of Wisconsin

Received: Jan 3, 2017

Revised: May 8, 2017

Accepted: May 19, 2017

## INTRODUCTION

SEC23 is a core component of coat protein complex II (COPII) vesicles, which transport secretory proteins from the endoplasmic reticulum (ER) to the Golgi apparatus. The genes encoding COPII vesicle components are highly evolutionarily conserved; however, in contrast to yeast, the mammalian genome contains two or more paralogues for most of these genes (Bonifacino and Glick, 2004; Khoriaty *et al.*, 2012; Zanetti *et al.*, 2012). The two mammalian

paralogues for SEC23—SEC23A and SEC23B—exhibit ~85% amino acid sequence identity (Bonifacino and Glick, 2004; Khoriaty *et al.*, 2012; Zanetti *et al.*, 2012). In humans, SEC23A mutations result in cranio-lenticulo-sutural dysplasia, an autosomal recessive disease characterized by late closure of fontanelles, skeletal abnormalities, and sutural cataracts (Boyadjiev *et al.*, 2010; Lang *et al.*, 2006), whereas homozygous/compound heterozygous loss-of-function SEC23B mutations result in congenital dyserythropoietic anemia type II (CDAll; Bianchi *et al.*, 2009; Schwarz *et al.*, 2009; Khoriaty *et al.*, 2012), a disease characterized by a defect in erythroid maturation. We previously reported that mice genetically deficient for SEC23A exhibit midembryonic lethality and a cranial developmental defect (Zhu *et al.*, 2015), and mice homozygous for a *Sec23b* null allele die perinatally with massive pancreatic degeneration (Tao *et al.*, 2012). Mice with embryonic pancreas-specific SEC23B deficiency recapitulated the latter phenotype (Khoriaty *et al.*, 2016), with pancreas tissues harvested from these mice demonstrating abnormal acinar cell histology but normal-appearing islet cells.

The pancreas is a professional secretory organ with two highly active cell types engaged in protein synthesis and secretion—the exocrine acinar cell, which secretes digestive enzymes, and the endocrine beta and alpha cells, which secrete insulin and

This article was published online ahead of print in MBoC in Press (<http://www.molbiolcell.org/cgi/doi/10.1091/mbc.E17-01-0001>) on May 24, 2017.

Present addresses: <sup>†</sup>Department of Biology, Eastern Michigan University, Ypsilanti, MI 48197; <sup>‡</sup>Department of Ophthalmology, University of California, San Francisco, San Francisco, CA 94143; <sup>§</sup>Department of Oncology, Wayne State University School of Medicine, Detroit, MI 48201.

\*Address correspondence to: John A. Williams ([jawillms@med.umich.edu](mailto:jawillms@med.umich.edu)), David Ginsburg ([ginsburg@umich.edu](mailto:ginsburg@umich.edu)).

Abbreviations used: CDAll, congenital dyserythropoietic anemia type II; COPII, coat protein complex II; CreErT, tamoxifen-inducible Cre recombinase transgene; ER, endoplasmic reticulum; RER, rough endoplasmic reticulum; UPR, unfolded protein response; WT, wild type.

© 2017 Khoriaty *et al.* This article is distributed by The American Society for Cell Biology under license from the author(s). Two months after publication it is available to the public under an Attribution–Noncommercial–Share Alike 3.0 Unported Creative Commons License (<http://creativecommons.org/licenses/by-nc-sa/3.0>).

“ASCB®,” “The American Society for Cell Biology®,” and “Molecular Biology of the Cell®” are registered trademarks of The American Society for Cell Biology.

glucagon, respectively. Acinar cells contain abundant rough endoplasmic reticulum (RER), prominent Golgi, and large secretory granules termed zymogen granules (ZGs; Gorelick and Jamieson, 2012). Approximately 20 different digestive enzymes are synthesized on the RER and traverse the secretory pathway, with the ER to Golgi being a major concentrating step (Oprins et al., 2001). The early steps by which coated vesicles bud from smooth regions of the ER termed transition zones appear similar in acinar cells and other secretory cells. The concentrations of amylase and chymotrypsinogen are similar in the COPII vesicle and the RER lumen, suggesting a bulk flow process for this initial step (Martinez-Menarguez et al., 1999; Klumperman, 2000; Barlowe and Helenius, 2016).

To test whether SEC23B is required for normal pancreatic function in adult mice, we now report the characterization of mice with tamoxifen-inducible, acinar cell-specific SEC23B deficiency. Tamoxifen administration to adult mice results in loss of pancreatic mass with evidence of cell loss, degeneration of exocrine cells (with smaller-than-normal zymogen granules and ER dilation), ER stress, and increased pancreatic cell apoptosis.

## RESULTS

### Generation of mice with tamoxifen-inducible, pancreatic acinar cell-specific *Sec23b* deletion

Mice with tamoxifen-inducible, acinar cell-specific deletion of *Sec23b* were generated by crossing *Sec23b<sup>+/-</sup> CreErT<sup>+</sup>* mice to *Sec23b<sup>+fl</sup>* mice. This cross yielded the expected number of *Sec23b<sup>-fl</sup> CreErT<sup>+</sup>* mice at weaning (Table 1). One week after tamoxifen administration, pancreas tissues were harvested from the latter mice to determine the degree of excision of *Sec23b*. *Sec23b<sup>-fl</sup> CreErT<sup>+</sup>* pancreata exhibited ~90% lower expression of wild-type (WT) *Sec23b* mRNA by quantitative RT-PCR (qRT-PCR) than WT pancreata (Figure 1B), with similar decreases in steady-state SEC23B protein by Western blot analysis (Figure 1, C and D). Because CreErT is expressed only in acinar cells (Ji et al., 2008), some or all of the residual SEC23B expression could be derived from islet and other nonacinar cells. Thus these data are consistent with high-level excision of *Sec23b* in pancreatic acinar cells after tamoxifen administration. *Sec23a* mRNA and protein levels were not increased in pancreata of mice with acinar cell deletion of *Sec23b* (Figure 1, E–G).

### Depletion of *Sec23b* in acinar cells of adult mice results in lower pancreatic weight

One week after tamoxifen administration, mice were killed and pancreata were dissected and weighed. Mice with acinar cell deletion of *Sec23b* (*Sec23b<sup>-fl</sup> CreErT<sup>+</sup>* or *Sec23b<sup>fl/fl</sup> CreErT<sup>+</sup>* mice) exhibited ~40% decrease in pancreatic weight compared with WT control mice (*Sec23b<sup>fl/fl</sup> CreErT<sup>-</sup>*, *Sec23b<sup>+fl</sup> CreErT<sup>-</sup>*, *Sec23b<sup>+/+</sup> CreErT<sup>+</sup>*,

and *Sec23b<sup>+/+</sup> CreErT<sup>-</sup>* mice;  $p < 0.0001$ ), whereas pancreatic weights of mice with heterozygous acinar cell deletion of *Sec23b* (*Sec23b<sup>+/-</sup> CreErT<sup>+</sup>*, *Sec23b<sup>+/-</sup> CreErT<sup>-</sup>*, and *Sec23b<sup>+fl</sup> CreErT<sup>+</sup>* mice) were not significantly different than those of WT mice ( $p = 0.09$ ; Figure 2A).

The mouse weights before and after tamoxifen administration were indistinguishable between mice with acinar depletion of SEC23B and WT control mice (Figure 2, B and C), suggesting no effect of acinar *Sec23b* deletion on food intake or duodenal pathology.

To determine the baseline CreErT activity in the absence of tamoxifen induction, we gavaged a cohort of mice (*Sec23b<sup>-fl</sup> CreErT<sup>+</sup>*, *Sec23b<sup>fl/fl</sup> CreErT<sup>+</sup>*, and WT controls) with corn oil not containing tamoxifen. *Sec23b<sup>-fl</sup> CreErT<sup>+</sup>* and *Sec23b<sup>fl/fl</sup> CreErT<sup>+</sup>* mice exhibited ~13% lower pancreatic weights than WT mice ( $p = 0.03$ ; Figure 2D), explaining only a portion of the decrease in pancreatic weight observed in *Sec23b<sup>-fl</sup> CreErT<sup>+</sup>* and *Sec23b<sup>fl/fl</sup> CreErT<sup>+</sup>* mice after tamoxifen administration.

To determine whether the pancreatic weight after *Sec23b* acinar cell deletion would drop further with time, we followed a cohort of mice for 2 wk after administration of tamoxifen. The latter mice exhibited a ~40% decrease in pancreas weight compared with WT control mice (Figure 2 E), which is indistinguishable from the drop observed 1 wk after tamoxifen administration.

### The lower pancreatic weight in mice with acinar deletion of *Sec23b* is due to cell loss

We calculated total pancreatic DNA, RNA, and protein contents 1 wk after tamoxifen administration. Mice with acinar cell deletion of *Sec23b* exhibited ~43% decrease in pancreatic DNA content ( $p = 0.01$ ; Figure 2F), ~53% decrease in RNA content ( $p < 0.0001$ ; Figure 2G), and ~46% decrease in protein content ( $p < 0.0001$ ; Figure 2H) compared with WT mice. The total DNA, RNA, and protein contents of pancreas tissues decreased proportionately to the decrease in pancreas weights resulting from *Sec23b* deletion in acinar cells, indicating that the decreased pancreas weight can be fully explained by a reduction in cell number, not cell size.

### Acinar *Sec23b* deletion results in degeneration of exocrine cells, decreased zymogen granules, and ER alterations

One week after acinar cell-specific deletion of *Sec23b*, histologic evaluation of pancreas tissues demonstrated smaller-than-normal pancreata with mild to moderate disruption of normal lobular architecture due to multifocal degeneration of exocrine epithelial cells within pancreatic lobules, with shrinkage of lobules and prominence of supporting stroma and periductular fibrosis. Degenerate acinar cells were shrunken, with loss of zymogen granules, condensed nuclei, and cytoplasmic enhancement of the eosin stain (Figure 3A). Histologic evaluation of pancreas tissues performed 2 wk after

Genotype	<i>Sec23b<sup>+/+</sup> CreErT(+)</i>	<i>Sec23b<sup>+/+</sup> CreErT(-)</i>	<i>Sec23b<sup>+fl</sup> CreErT(+)</i>	<i>Sec23b<sup>+fl</sup> CreErT(-)</i>	<i>Sec23b<sup>+/-</sup> CreErT(+)</i>	<i>Sec23b<sup>+/-</sup> CreErT(-)</i>	<i>Sec23b<sup>-fl</sup> CreErT(+)</i>	<i>Sec23b<sup>-fl</sup> CreErT(-)</i>	p value <sup>a</sup>
Expected ratio (%)	12.5	12.5	12.5	12.5	12.5	12.5	12.5	12.5	
Percentage observed at weaning (n = 174)	9 (16)	13 (23)	14 (24)	14 (24)	13 (22)	13 (23)	11 (19)	13 (23)	>0.8

<sup>a</sup>p calculated for *Sec23b<sup>-fl</sup> CreErT(+)* mice versus all other genotypes.

**TABLE 1:** Results of *Sec23b<sup>+/-</sup> CreErT(+)* x *Sec23b<sup>+fl</sup>* matings to generate mice with tamoxifen-inducible, acinar cell-specific deletion of *Sec23b*.

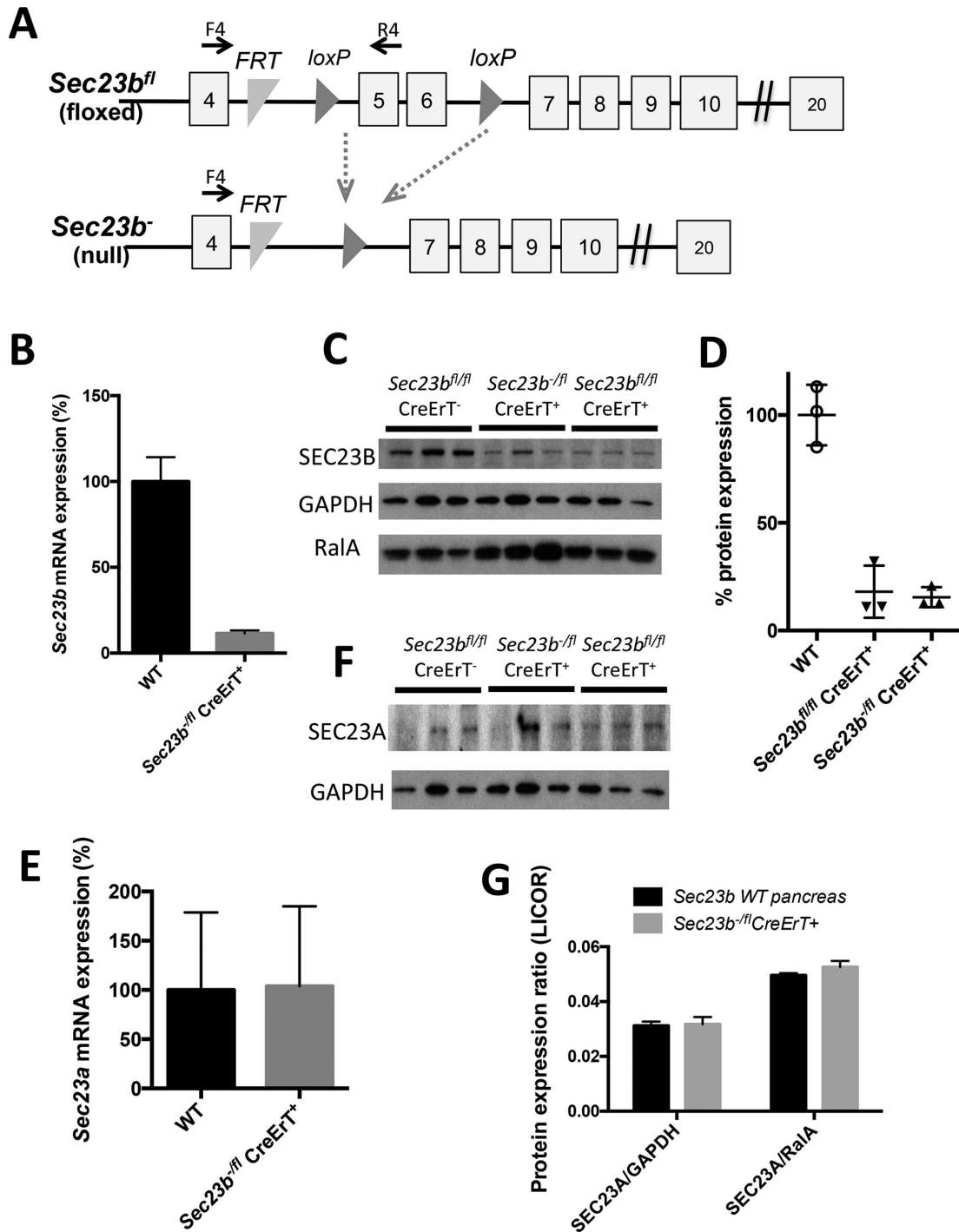


**FIGURE 1:** *Sec23b* inactivation in pancreatic acinar cells. (A) *Sec23b* alleles (not drawn to scale; Khoriaty *et al.*, 2014). Each square indicates an exon, and horizontal lines between exons indicate introns. F4 and R4 are primers used for assessing efficiency of Cre-mediated excision. (B) *Sec23b* excision determined by qPCR ( $n = 3$  for each genotype) and (C) Western blot on pancreas tissues 7 d after administration of tamoxifen. (D) Quantification of the SEC23B band intensities in C relative to average of GAPDH and RalA performed using ImageJ. (E–G) Quantitation of *Sec23a* expression by (E) qPCR (three controls and four *Sec23b<sup>fl/fl</sup> CreErT<sup>+</sup>* mice), (F) chemiluminescence Western blot detection, and (G) quantitative Western blot (infrared fluorescence detection) in pancreas tissues 7 d after administration of tamoxifen (three mice per genotype).

tamoxifen administration revealed comparable findings (Supplemental Figure S1A).

Alteration in acinar morphology after *Sec23b* excision was also assessed by electron microscopy (Figure 4). Seven days after

tamoxifen treatment, acinar cell structure in pancreata of WT mice exhibited the expected concentration of zymogen granules surrounding the acinar lumen in the apical pole of the cell and abundant RER in basolateral regions (Figure 4A). In contrast, the majority

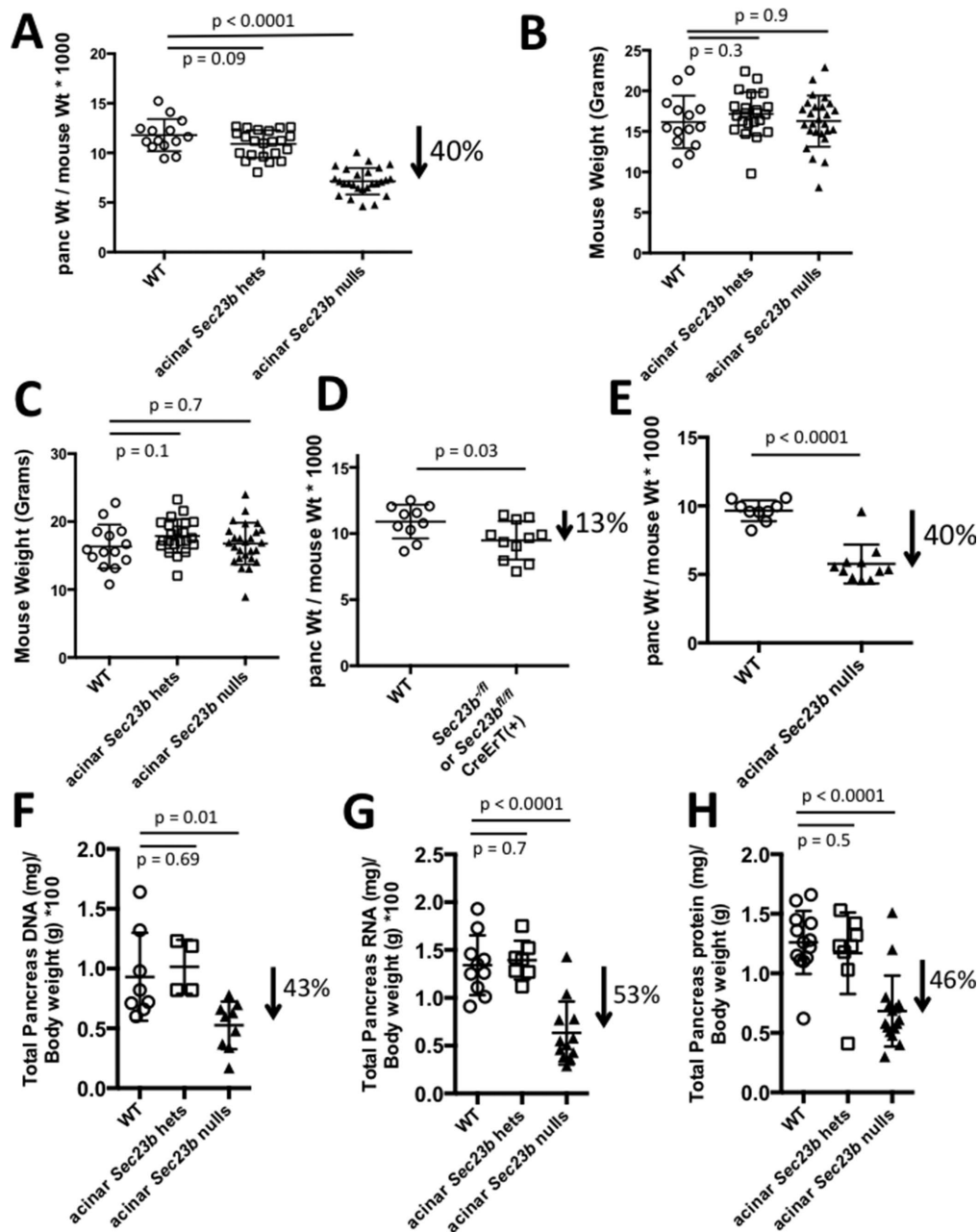


**FIGURE 2:** *Sec23b* deletion in acinar cells results in decreased pancreatic weight from cell loss. (A) Ratios of pancreas to total body weight 7 d after administration of tamoxifen indicate substantial loss of pancreas weight resulting from inactivation of *Sec23b* in pancreas acinar cells. Mouse weights (B) before and (C) 1 wk after tamoxifen administration indicates no loss of total body weight with acinar deletion of *Sec23b*. (D) Ratios of pancreas to total body weight 7 d after administration of corn oil demonstrate that only a small portion of the pancreatic weight loss is explained by basal CreErT activity in the absence of tamoxifen induction. (E) A cohort of mice were evaluated 14 d after tamoxifen administration, demonstrating no continued drop in pancreatic weight compared with evaluation performed 7 d after tamoxifen in A. The loss of pancreatic weight is associated with a comparable degree of decrease in pancreas (F) DNA, (G) RNA, and (H) total protein, consistent with cell loss. Each data point represents one mouse.

of acinar cells in *Sec23b<sup>fl/fl</sup>* CreErT<sup>+</sup> mice exhibited striking abnormalities, including decreased zymogen granules (Figure 4) and alterations in ER morphology ranging from vesicular ER to markedly expanded cisternae with accumulation of moderate-density content or intracisternal granules (Figure 4, B–F). Cells containing vesicular ER often showed ribosomes associated with only portions of the

vesicular membrane (Figure 4, F and inset). Many acinar cells showed alteration in their general polarity, with granules accumulating in basal regions of the cell, whereas other cells had greatly reduced granule densities. The acinar cell morphology was also assessed 14 d after administration of tamoxifen, with findings similar to those at the earlier time point (Supplemental Figure S2).

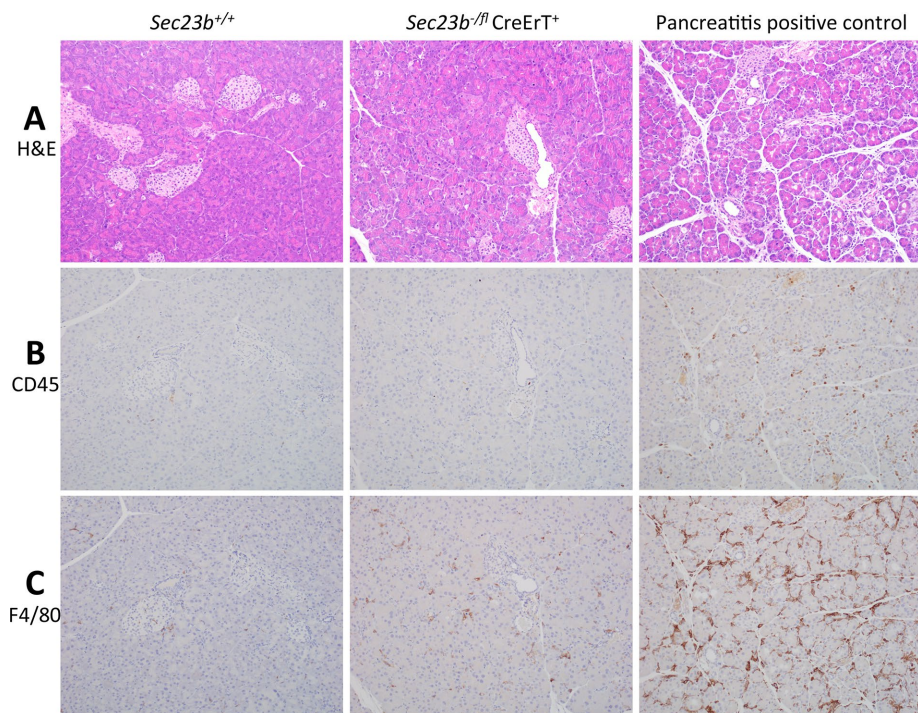


**FIGURE 3:** Histologic evaluation of pancreas tissues 7 d after deletion of acinar *Sec23b*. The evaluation was performed by an investigator blinded to the genotypes of the mice from which the tissues were derived (four mice of each genotype were evaluated). (A) At 7 d after acinar *Sec23b* deletion, evaluation of pancreas tissues by hematoxylin and eosin stains demonstrated overall loss of parenchymal size and lobular atrophy due to degeneration of acinar epithelial cells, characterized by cellular shrinkage, cytoplasmic loss with loss of zymogen granules, enhancement of the eosin stain, and nuclear pyknosis (middle) compared with WT controls (left). Right, positive control for pancreatitis 1 d after cerulean treatment. Immunohistochemistry for (B) CD45 and (C) F4/80 demonstrates a small number of white blood cells (mostly macrophages) infiltrating pancreas tissues of mice with acinar *Sec23b* deletion compared with mice with cerulean-induced pancreatitis (positive control).

### ***Sec23b* deletion in acinar cells fails to produce clear manifestations of acute pancreatitis**

We measured random blood glucose and plasma amylase levels 1 wk after tamoxifen administration. Mice with acinar cell deletion of *Sec23b* exhibited indistinguishable blood glucose (Figure 5A) and plasma amylase levels (Figure 5B) compared with mice heterozygous for *Sec23b* in their acinar cells and WT controls. In addition, a small number of white blood cells (mostly resident macrophages and lymphocytes) were observed by immunohistochemistry, but much fewer than in the pancreatitis positive control samples, which contained a significant number of neutrophils in addition to large numbers of other inflammatory cells (Figure 3, B and C, and Supplemental Figure S1, B and C). Carboxypeptidase A1 cleavage, which is seen in pancreatitis (Leach *et al.*, 1991), was not observed in pancreas tissues of mice with acinar *Sec23b* deletion (Figure 5C). Other pancreas digestive enzymes were variably affected relative to total protein. Amylase was decreased in total pancreatic cell lysates prepared from mice with acinar deletion of *Sec23b* compared with WT mice (Figure 5D), with a less clear effect on chymotrypsin and trypsin (Figure 5E).

### **Acinar *Sec23b* deletion results in ER stress and increased apoptosis**

To determine whether the ER dilatation observed after acinar *Sec23b* deletion is associated with induction of ER stress and the unfolded protein response (UPR), we determined the expression level of a

panel of associated genes by qRT-PCR. Expression for many of these genes was increased after acinar *Sec23b* deletion, with the increase in *Eif2a* and *Grp94* reaching statistical significance ( $p < 0.05$ ; Figure 6A).

After tamoxifen administration, terminal deoxynucleotidyl transferase dUTP nick end labeling (TUNEL) assays were also performed on pancreatic tissues harvested from *Sec23b*<sup>-/-</sup> CreErT<sup>+</sup> mice and WT controls (Figure 6B, a–d). Three days after tamoxifen administration, the percentage of TUNEL-positive cells in *Sec23b*<sup>-/-</sup> CreErT<sup>+</sup> mice (6.08%) was higher than that in WT control mice (0.04%; Figure 6C). The same pattern was observed 7 d after tamoxifen administration (1.62 and 0.11%, respectively; Figure 6C). Consistent with these results, the expression of activated caspase 3 was increased in pancreata of *Sec23b*<sup>-/-</sup> CreErT<sup>+</sup> mice compared with WT control mice (Figure 6B, e and f).

## **DISCUSSION**

Mice with germline deletion of *Sec23b* die perinatally, exhibiting massive pancreatic degeneration (Tao *et al.*, 2012). Pancreas-specific *Sec23b* deletion in developing mouse embryos recapitulates the phenotype of mice with global SEC23B deficiency (Khoriaty *et al.*, 2016), demonstrating that the defect in the latter mice is intrinsic to the pancreas. It is not clear whether this effect is mediated by the loss of the endocrine or exocrine pancreas or the development of intrauterine pancreatitis.

In this study, we evaluated the effect of SEC23B depletion in adult pancreatic acinar cells by generating mice with tamoxifen-inducible, acinar cell-specific SEC23B deficiency. Tissue was evaluated from 3 d to 2 wk after tamoxifen. Tamoxifen administration to these adult mice results in pancreatic cell loss, swollen ER with degeneration of exocrine cells, ER stress, and increased pancreatic acinar cell apoptosis but without an effect on viability of the mice. There were small numbers of white blood cells (primarily resident macrophages and lymphocytes) in pancreatic tissues of the latter mice; these infiltrates were minimal in comparison to the moderate inflammatory cell infiltration in the pancreatitis-positive control tissues. In addition, the pancreatitis control tissues exhibited a significant number of neutrophils, consistent with a primary inflammatory process in the pancreas. In contrast, the small numbers of macrophages observed in the pancreas of SEC23B-depleted mice is consistent with a clean-up process secondary to acinar degeneration rather than an active inflammatory process. In addition, amylase was not increased in the plasma of mice with acinar depletion of SEC23B, and carboxypeptidase cleavage was not observed, arguing against frank pancreatitis. Taken together, these data demonstrate that SEC23B is important for maintenance of function of adult murine pancreatic acinar cells. Specifically, the results are consistent with a role for SEC23B in forming the COPII coat, which promotes budding of transport vesicles off the ER, initiating passage through the secretory pathway and culminating in the production of ZG. Blockage of the early secretory pathway explains the reduction in ZG. Because some granules are still present, the

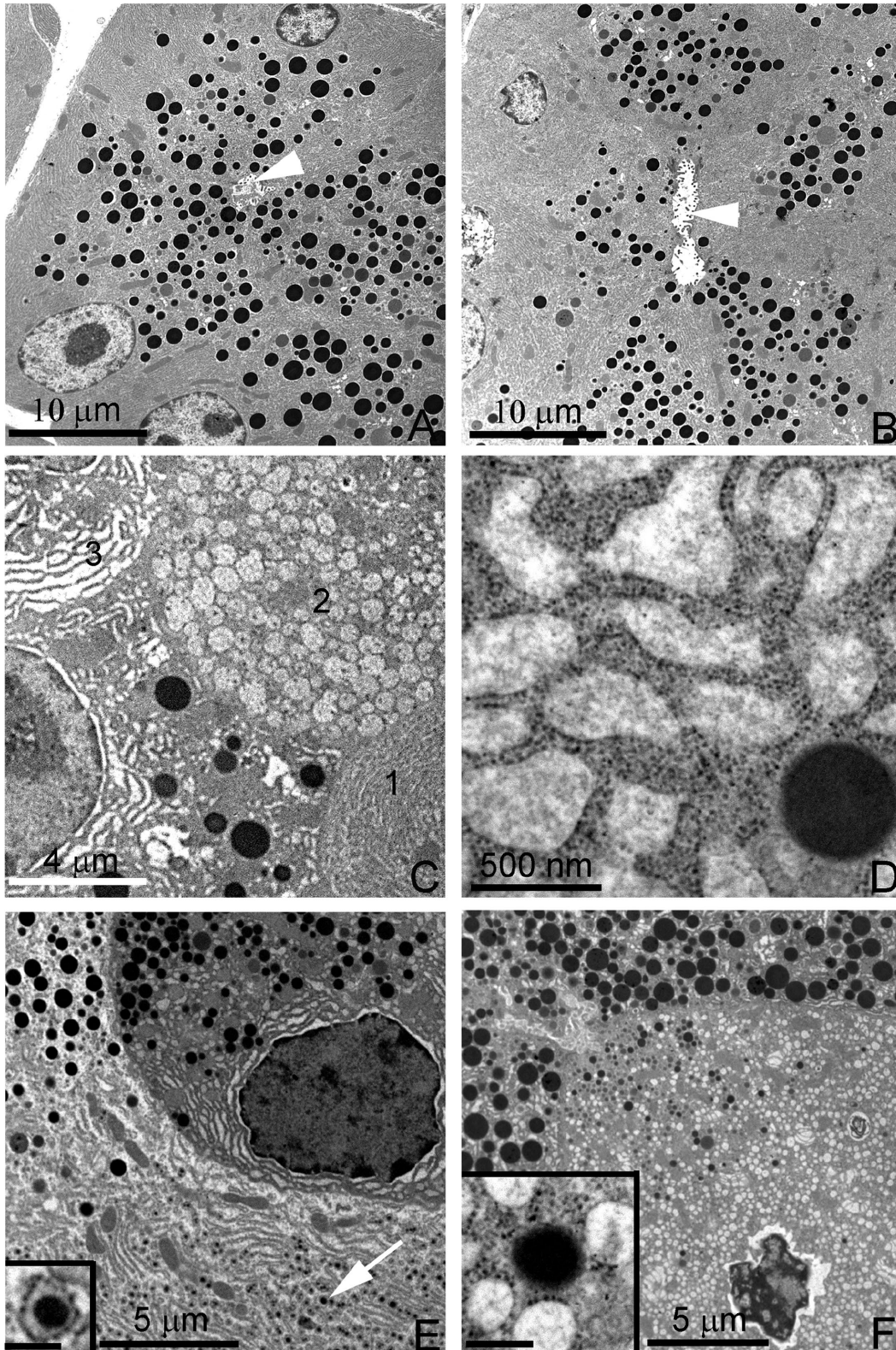


**FIGURE 4:** Electron microscopy of pancreas tissues 7 d after deletion of acinar *Sec23b*. Evaluation of pancreas tissues by electron microscopy demonstrates normal acinar morphology in WT control mice, with numerous granules adjacent to the lumen (arrowhead) and basal RER cisternae (A). Pancreas tissues with acinar deletion of *Sec23b* exhibited variably decreased zymogen granules (B; arrowhead denotes ER lumen), as well as multiple alterations, including vesicular or expanded RER (C, cells 2 and 3; in contrast to normal cell morphology, C, cell 1), expanded RER cisternae with amorphous content (C, D), small intracisternal granules (E, arrow and higher-magnification inset), crenulated nucleus and vesicular RER (F), with amorphous content and partial studding with ribosomes (F and inset). Scale bars as indicated; 250 nm (insets). Three mice of each genotype were evaluated.

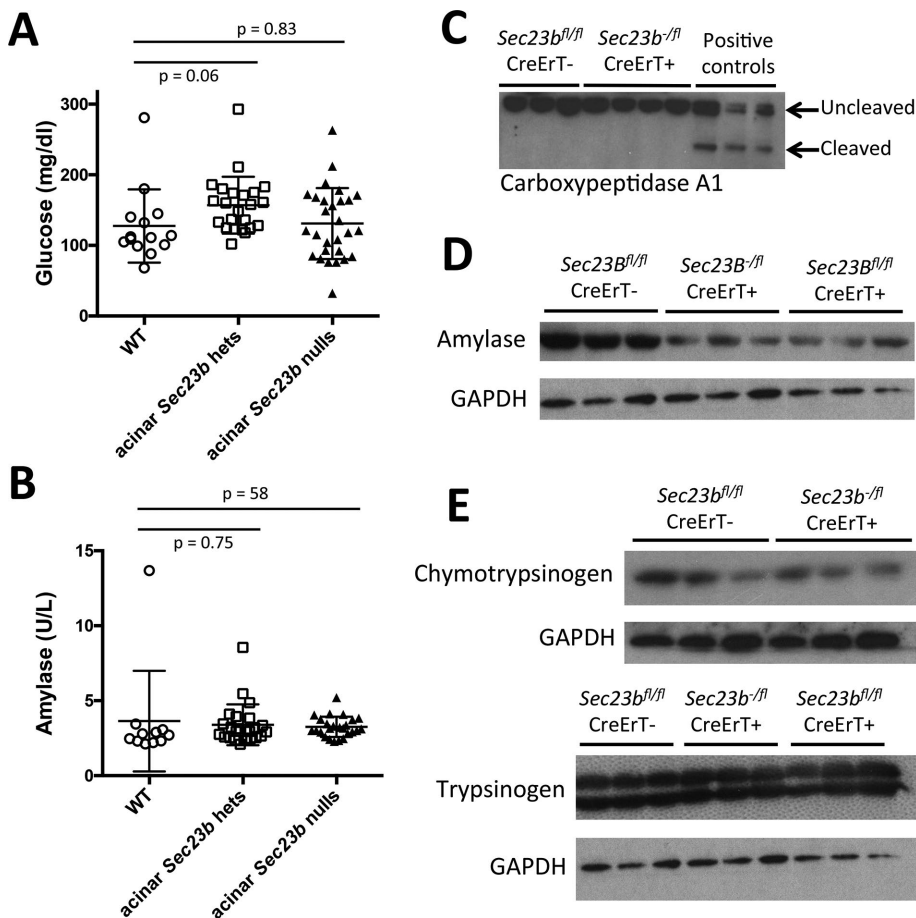


**FIGURE 5:** Deletion of *Sec23b* in mouse acinar cells does not affect plasma glucose or amylase but results in decreased pancreatic amylase in total pancreas cell lysates. (A) *Sec23b* deletion in acinar cells does not result in increased plasma glucose or (B) increased plasma amylase (each data point represents one mouse). (C) Carboxypeptidase cleavage observed in pancreas tissues of mice given cerulein to induce pancreatitis was not observed in pancreas tissues of mice with acinar *Sec23b* inactivation. (D) *Sec23b* deletion in pancreas acinar cells results in decreased pancreatic amylase in total pancreas cell lysates, (E) with a less clear effect on chymotrypsin and trypsin.

blockage is not complete. Of interest, different digestive enzymes move through the pathway to the ZG at different rates. Chymotrypsinogen moves faster and shows a higher increase in concentration than amylase (Oprins *et al.*, 2001). The slower movement of amylase may be related to the overall fall in tissue amylase compared with chymotrypsinogen, which does not fall in SEC23B deficiency.

In contrast to mice with germline SEC23B deficiency, *Sec23b* deletion in pancreatic acinar cells of adult mice is not lethal (a cohort of mice was followed for ~2–3 wk after tamoxifen administration). One possible explanation is that these mice were observed for too short a time after tamoxifen administration to assess for mortality. Alternatively, selection over time against acinar cells with complete *Sec23b* excision could result in enrichment for normal acinar cells with intact *Sec23b*. Another possible explanation is that the small percentage of acinar cells without *Sec23b* excision might be sufficient for survival of these mice. It is also possible that *Sec23b* exerts a unique function during murine embryonic development, which is responsible for the damage in the setting of germline deletion.

Acinar cell death after *Sec23b* deletion could result from accumulation of exocrine pancreatic enzymes in the ER, resulting in ER stress and apoptosis. Consistent with this hypothesis, mutations in *PRSS1*, the gene encoding trypsinogen, that result in an increase of its activ-

ity have been associated with pancreatitis (Whitcomb *et al.*, 1996a,b; Ferec *et al.*, 1999). Similarly, mutation in *SPINK1*, which encodes a serine protease with antitrypsin activity, is associated with hereditary pancreatitis (Witt *et al.*, 2000; Audrezet *et al.*, 2002). However, these genes are involved in enhancing or inhibiting the activity of trypsin while still in the acinar cell. Deletion of SEC23B inhibits exit from the ER but is not expected to affect trypsin activation and for this reason may not promote pancreatitis in the adult mouse. Variants in procarboxypeptidase A1 in humans were shown to be associated with pancreatitis associated with ER stress but without trypsin activation (Witt *et al.*, 2013). Further work on the type of ER stress induced by *Sec23b* deletion in murine acinar cells is warranted.

## MATERIALS AND METHODS

### Mice and PCR genotyping

A *Sec23b* floxed allele (*Sec23b<sup>fl</sup>*) and a *Sec23b* null allele (*Sec23b<sup>-</sup>*) were generated as previously described (Figure 1A; Khoriaty *et al.*, 2014). Mice carrying a pancreatic acinar cell-specific, tamoxifen-inducible Cre recombinase (CreErT) transgene (a generous gift from C. Logsdon, M.D. Anderson Cancer Center, Houston, TX; Ji *et al.*, 2008) were crossed to *Sec23b<sup>+/-</sup>* mice to generate *Sec23b<sup>+/-</sup>* CreErT<sup>+</sup> mice. CreErT mice express Cre recombinase under the control of the full-length elastase gene promoter, resulting in expression of Cre recombinase in nearly 100% of the acinar cells but not in duct or islet cells (Ji *et al.*, 2008; Gurda *et al.*, 2010). Genotyping for the *Sec23b<sup>fl</sup>*, *Sec23b<sup>-</sup>*, and CreErT alleles was performed as previously described (Ji *et al.*, 2008;

Khoriaty *et al.*, 2014). All of the mice used in this study were either generated on the C57BL/6J background or crossed to the latter genetic background for more than six generations.

A cohort of WT mice were given cerulein (50  $\mu$ g/kg) every hour for 7 h to induce pancreatitis as previously described (Sans *et al.*, 2003). These mice, which exhibit increased plasma amylase and pancreatic cell damage, were used as positive control for pancreatitis.

### Tamoxifen administration

Tamoxifen (purchased from Sigma-Aldrich) was dissolved in corn oil at 10 mg/ml. Mice at 5–6 wk of age were administered tamoxifen (3 mg tamoxifen per 40 g of mouse weight) via daily gavage for 4 d.

### Blood glucose and amylase measurement

Blood glucose was measured using the OneTouch Ultra glucometer (LifeScan) or the Contour glucometer (Bayer), and plasma amylase was measured using Phadebas reagents (MagLe Life Sciences) according to manufacturer's instructions.

### DNA, RNA, and protein isolation and measurement

Pancreas tissue samples were weighed and homogenized at 100 mg/1.5 ml solution of 5 mM MgCl<sub>2</sub> plus 0.1% Triton X-100 and then

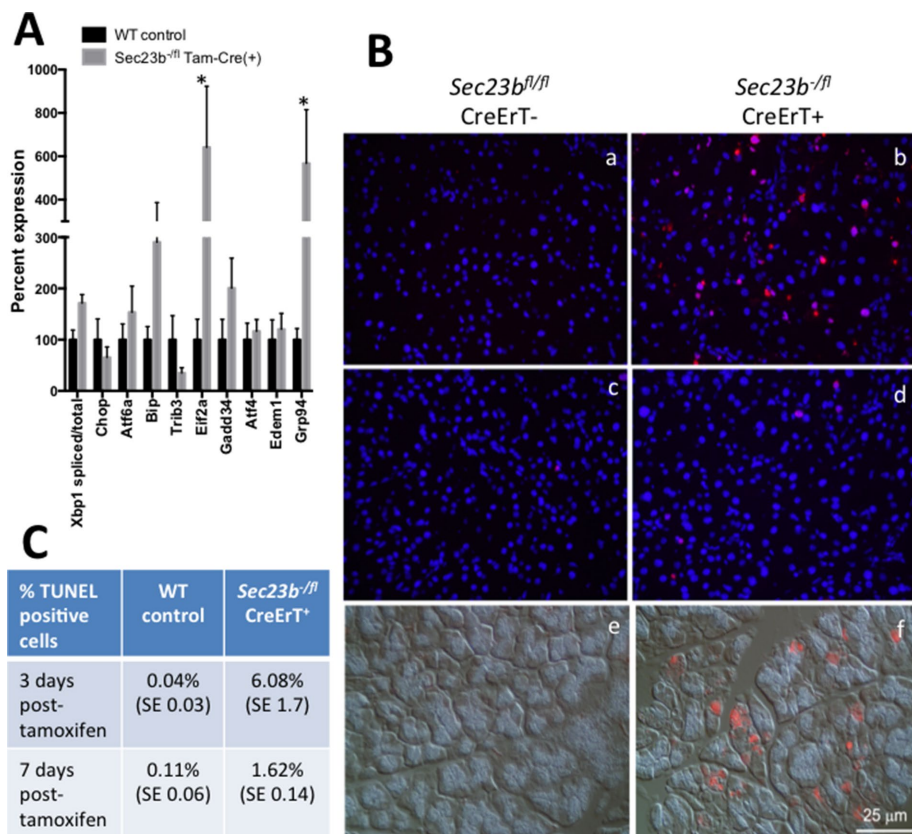


**FIGURE 6:** Expression of UPR genes and TUNEL assay in pancreas tissues after acinar *Sec23b* deletion. (A) Real time RT-PCR expression of select UPR genes was performed on pancreas tissues harvested 1 wk following administration of tamoxifen, with levels normalized to  $\beta$ -actin. Data are represented by mean  $\pm$  SEM. Asterisks indicate statistically significant difference between WT and *Sec23b*<sup>-/-</sup> CreErT(+) samples. Six mice from each genotype were evaluated. (B) TUNEL assays overlaid on DAPI were performed 3 d (a, b) and 7 d (c, d) after administration of tamoxifen. *Sec23b*<sup>-/-</sup> CreErT<sup>+</sup> mice exhibit increased apoptosis at both time points. Immunostaining for active caspase-3 demonstrates increased expression in mice with acinar deletion of *Sec23b* (f) compared with WT mice (e) on Nomarski image. (C) Average percentage of TUNEL-positive cells (three or four mice were evaluated per condition and ~2000–2500 cells counted per sample). The evaluation was performed by an investigator blinded to the genotypes of the mice from which the tissues were derived.

sonicated. DNA and RNA were measured using the Qubit RNA HS Assay Kit (Q32852; Life Technologies) and Qubit dsDNA HS Assay Kit (Q32851; Life Technologies), respectively, according to manufacturer's instructions. Protein was measured spectrophotometrically by using Bio-Rad protein assay reagent. Total pancreatic protein, DNA, and RNA were then calculated (Tashiro *et al.*, 2004; Crozier *et al.*, 2010).

#### qRT-PCR

RNA was isolated from pancreas tissues using the RNeasy Kit (Qiagen). cDNA synthesis was carried out using the Superscript First-Strand Synthesis System for RT-PCR (Invitrogen) with random primers. Power SYBR Green PCR Master Mix (Applied Biosystems) was used for qRT-PCR using the Applied Biosystems 7900HT Fast Real-Time PCR System. Each sample was analyzed in triplicate, and *Gapdh* (glyceraldehyde-3-phosphate dehydrogenase) or *Atcb* ( $\beta$ -actin) was used as internal control. Relative gene expression was determined using the  $2^{-\Delta\Delta CT}$  method. Supplemental Table S1 lists primers used.

#### Western blot and antibodies

Total cell lysates were prepared from pancreas tissues, and Western blots (film visualization with chemiluminescence detection) were

performed as previously described (Khoriaty *et al.*, 2014). Mouse anti-actin and anti-GAPDH antibodies were obtained from Santa Cruz Biotechnology and Millipore, respectively. Rabbit anti-SEC23B and anti-SEC23A antibodies were generated as previously described (Khoriaty *et al.*, 2014). Carboxypeptidase A1, amylase, chymotrypsin, and trypsin antibodies were obtained from R&D Systems (AF2765), Sigma-Aldrich (A8273), Fitzgerald (20C-CR1095R), and Santa Cruz Biotechnology (sc-67388), respectively. Quantitative Western blots (infrared fluorescence detection) were performed and analyzed as previously described (Khoriaty *et al.*, 2016).

#### Hematoxylin and eosin staining and electron microscopy

Pancreas tissues were collected and fixed in 4% paraformaldehyde for histologic analysis. Tissues were processed, embedded in paraffin, sectioned at 4  $\mu$ m, and stained with hematoxylin and eosin. Electron microscopy was performed on pancreas tissues as previously described (Crozier *et al.*, 2009; Hou *et al.*, 2015). In brief, minced pancreas was fixed in a mixture of 2% formaldehyde and 2% glutaraldehyde in phosphate-buffered saline, postfixed in 1% osmium tetroxide, and then dehydrated and embedded in Epon. Ultrathin sections were stained with uranyl acetate and lead citrate and evaluated with a Phillips CM-100 electron microscope.

#### Immunohistochemistry

Immunohistochemistry was performed as previously described (Khoriaty *et al.*, 2016) with anti-CD45 and anti-F4/80 antibodies purchased from Novus Biologicals (NB100-77417) and Abcam (ab6640), respectively.

#### TUNEL assay and caspase 3 immunostaining

The ApopTag Red In Situ Apoptosis Detection Kit (Chemicon, Millipore) was used to localize red fluorescent TUNEL-positive nuclei. Briefly, fresh-frozen sections of pancreas were fixed for 10 min with a 2:1 mixture of methanol and acetone at  $-20^{\circ}\text{C}$ . Sections were treated with the kit reagents as specified by the manufacturer, coverslipped with mounting medium containing fluorescent nuclear stain 4',6-diamidino-2-phenylindole (DAPI; Prolong Gold, Invitrogen), and viewed with a 40x objective of an Olympus BX-51 fluorescence microscope. Five randomly chosen DAPI-stained fields in sections from each animal were photographed, each followed by changing filters to photograph TUNEL fluorescence. DAPI-stained nuclei were counted using the Nuclei Counting program in MetaMorph software (Molecular Devices, Sunnyvale, CA), and TUNEL-positive nuclei were counted manually. The percentage of TUNEL-positive nuclei was calculated for each field (five determinations per mouse), and these values were then averaged for each mouse. This experiment was performed by an investigator blinded to the genotypes of the mice from which the pancreas tissues were harvested.

Immunofluorescence localization of caspase-3 (8G10 rabbit monoclonal antibody, Cell Signaling Technology, Danvers, MA;

Alexa anti-rabbit 594, Thermo Fisher Scientific, Grand Island, NY) was performed on cryostat sections of pancreas tissue that had been fixed in 4% paraformaldehyde. Immunostaining for caspase-3 was merged with its corresponding Nomarski image to show acinar cell distribution of caspase-3.

### Statistical analysis

The chi-square test was used to determine the statistical significance of the deviation from Mendelian ratios for mouse crosses. The Student's *t* test was used to calculate the statistical significance of the differences between various parameters among different genotype groups. *p* < 0.05 is considered statistically significant.

### ACKNOWLEDGMENTS

We acknowledge Elizabeth Hughes, Keith Childs, and Thomas Saunders for preparation of gene-targeted mice and the Transgenic Animal Model Core of the University of Michigan's Biomedical Research Core Facilities. This work was supported by National Institutes of Health Grants R01 HL039693 and P01-HL057346 (D.G.), K08 HL128794 (R.K.), and R37-DK041122 (J.A.W.). R.K. is the recipient of an American Society of Hematology Scholar Award. D.G. is a Howard Hughes Medical Institute investigator. Core support was provided by the University of Michigan Cancer Center (P30 CA046592) and Michigan Gastrointestinal Peptide Center (P30 DK34933).

### REFERENCES

Audrezet MP, Chen JM, Le Marechal C, Ruzsniwski P, Robaszkiwicz M, Raguene O, Quere I, Scotet V, Ferec C (2002). Determination of the relative contribution of three genes—the cystic fibrosis transmembrane conductance regulator gene, the cationic trypsinogen gene, and the pancreatic secretory trypsin inhibitor gene—to the etiology of idiopathic chronic pancreatitis. *Eur J Hum Genet* 10, 100–106.

Barlowe C, Helenius A (2016). Cargo capture and bulk flow in the early secretory pathway. *Annu Rev Cell Dev Biol* 32, 197–222.

Bianchi P, Fermo E, Vercellati C, Boschetti C, Barcellini W, Iurlo A, Marcello AP, Righetti PG, Zanella A (2009). Congenital dyserythrocytic anemia type II (CDAIL) is caused by mutations in the SEC23B gene. *Hum Mutat* 30, 1292–1298.

Bonifacino JS, Glick BS (2004). The mechanisms of vesicle budding and fusion. *Cell* 116, 153–166.

Boyadjev SA, Kim SD, Hata A, Haldeman-Englert C, Zackai EH, Naydenov C, Hamamoto S, Schekman RW, Kim J (2010). Cranio-lenticulo-sutural dysplasia associated with defects in collagen secretion. *Clin Genet* 80, 169–176.

Crozier SJ, D'Alecy LG, Ernst SA, Ginsburg LE, Williams JA (2009). Molecular mechanisms of pancreatic dysfunction induced by protein malnutrition. *Gastroenterology* 137, 1093–1101. e3.

Crozier SJ, Sans MD, Wang JY, Lentz SI, Ernst SA, Williams JA (2010). CCK-independent mTORC1 activation during dietary protein-induced exocrine pancreas growth. *Am J Physiol Gastrointest Liver Physiol* 299, G1154–G1163.

Ferec C, Raguene O, Salomon R, Roche C, Bernard JP, Guillot M, Quere I, Faure C, Mercier B, Audrezet MP, et al. (1999). Mutations in the cationic trypsinogen gene and evidence for genetic heterogeneity in hereditary pancreatitis. *J Med Genet* 36, 228–232.

Gorelick F, Jamieson J (2012). Structure-function relationship in the pancreatic acinar cell. In: *Physiology of the Gastrointestinal Tract*, ed. L Johnson, San Diego, CA: Academic Press, 1341–1360.

Guirda GT, Crozier SJ, Ji B, Ernst SA, Logsdon CD, Rothermel BA, Williams JA (2010). Regulator of calcineurin 1 controls growth plasticity of adult pancreas. *Gastroenterology* 139, 609–619, 619.e1–6.

Hou Y, Ernst SA, Stuenkel EL, Lentz SI, Williams JA (2015). Rab27A is present in mouse pancreatic acinar cells and is required for digestive enzyme secretion. *PLoS One* 10, e0125596.

Ji B, Song J, Tsou L, Bi Y, Gaiser S, Mortensen R, Logsdon C (2008). Robust acinar cell transgene expression of CreErT via BAC recombineering. *Genesis* 46, 390–395.

Khoriati R, Everett L, Chase J, Zhu G, Hoenerhoff M, McKnight B, Vasievich MP, Zhang B, Tomberg K, Williams J, et al. (2016). Pancreatic SEC23B deficiency is sufficient to explain the perinatal lethality of germline SEC23B deficiency in mice. *Sci Rep* 6, 27802.

Khoriati R, Vasievich MP, Ginsburg D (2012). The COPII pathway and hematology disease. *Blood* 120, 31–38.

Khoriati R, Vasievich MP, Jones M, Everett L, Chase J, Tao J, Siemieniak D, Zhang B, Maillard I, Ginsburg D (2014). Absence of a red blood cell phenotype in mice with hematopoietic deficiency of SEC23B. *Mol Cell Biol* 34, 3721–3734.

Klumperman J (2000). Transport between ER and Golgi. *Curr Opin Cell Biol* 12, 445–449.

Lang MR, Lapierre LA, Frotscher M, Goldenring JR, Knapik EW (2006). Secretory COPII coat component Sec23a is essential for craniofacial chondrocyte maturation. *Nat Genet* 38, 1198–1203.

Leach SD, Modlin IM, Scheele GA, Gorelick FS (1991). Intracellular activation of digestive zymogens in rat pancreatic acini. Stimulation by high doses of cholecystokinin. *J Clin Invest* 87, 362–366.

Martinez-Menarguez JA, Geuze HJ, Slot JW, Klumperman J (1999). Vesicular tubular clusters between the ER and Golgi mediate concentration of soluble secretory proteins by exclusion from COPI-coated vesicles. *Cell* 98, 81–90.

Oprins A, Rabouille C, Posthuma G, Klumperman J, Geuze HJ, Slot JW (2001). The ER to Golgi interface is the major concentration site of secretory proteins in the exocrine pancreatic cell. *Traffic* 2, 831–838.

Sans MD, DiMaggio MJ, D'Alecy LG, Williams JA (2003). Caerulein-induced acute pancreatitis inhibits protein synthesis through effects on eIF2B and eIF4F. *Am J Physiol Gastrointest Liver Physiol* 285, G517–G528.

Schwarz K, Iolascon A, Verissimo F, Trede NS, Horsley W, Chen W, Paw BH, Hopfner KP, Holzmann K, Russo R, et al. (2009). Mutations affecting the secretory COPII coat component SEC23B cause congenital dyserythrocytic anemia type II. *Nat Genet* 41, 936–940.

Tao J, Zhu M, Wang H, Afelik S, Vasievich MP, Chen XW, Zhu G, Jensen J, Ginsburg D, Zhang B (2012). SEC23B is required for the maintenance of murine professional secretory tissues. *Proc Natl Acad Sci USA* 109, E2001–E2009.

Tashiro M, Samuelson LC, Liddle RA, Williams JA (2004). Calcineurin mediates pancreatic growth in protease inhibitor-treated mice. *Am J Physiol Gastrointest Liver Physiol* 286, G784–G790.

Whitcomb DC, Gorry MC, Preston RA, Furey W, Sossenheimer MJ, Ulrich CD, Martin SP, Gates LK Jr, Amann ST, Toskes PP, et al. (1996a). Hereditary pancreatitis is caused by a mutation in the cationic trypsinogen gene. *Nat Genet* 14, 141–145.

Whitcomb DC, Preston RA, Aston CE, Sossenheimer MJ, Barua PS, Zhang Y, Wong-Chong A, White GJ, Wood PG, Gates LK Jr, et al. (1996b). A gene for hereditary pancreatitis maps to chromosome 7q35. *Gastroenterology* 110, 1975–1980.

Witt H, Beer S, Rosendahl J, Chen JM, Chandak GR, Masamune A, Bence M, Szmola R, Orac G, Macek M, et al. (2013). Variants in CPA1 are strongly associated with early onset chronic pancreatitis. *Nat Genet* 45, 1216–1220.

Witt H, Luck W, Hennies HC, Classen M, Kage A, Lass U, Landt O, Becker M (2000). Mutations in the gene encoding the serine protease inhibitor, Kazal type 1 are associated with chronic pancreatitis. *Nat Genet* 25, 213–216.

Zanetti G, Pahuja KB, Studer S, Shim S, Schekman R (2012). COPII and the regulation of protein sorting in mammals. *Nat Cell Biol* 14, 20–28.

Zhu M, Tao J, Vasievich MP, Wei W, Zhu G, Khoriati RN, Zhang B (2015). Neural tube opening and abnormal extraembryonic membrane development in SEC23A deficient mice. *Sci Rep* 5, 15471.